Progress in Fractional Differentiation and Applications
An International Journal

http://dx.doi.org/10.18576/pfda/120109

Analysis of Cholera Model Transmission Dynamics Via Classical and ABC Fractional Derivatives

Tulu Leta Tirfe[1], *Legesse Lemecha Obsu*[2] *and Eshetu Dadi Gurmu* [2,*]

[1] Department of Mathematics, Bule Hora University, Bule Hora, Ethiopia
[2] Department of Applied Mathematics, Adama Science and Technology University, Adama, Ethiopia

Received: 2 Mar. 2025, Revised: 10 Apr. 2025, Accepted: 12 May. 2025
Published online: 1 Jan. 2026

Abstract: This study develops a mathematical model for cholera transmission dynamics using the Susceptible -Asymptomatic -Infected- Quarantined- Recovered- Bacterium formulation,incorporating both classical and Atangana-Baleanu fractional-order derivatives. The model is expressed as a system of fractional differential equations (FDEs) to characterize the non-local memory effects inherent in cholera transmission. The well-posedness of the model is established by proving the existence, uniqueness, and positivity of solutions using fixed-point theory. The basic reproduction number is derived via the next-generation matrix method, serving as a threshold parameter to determine disease persistence or eradication. Local and global stability analyses of equilibrium states are performed using the Jacobian matrix,Metzler matrix theory, and Lyapunov function techniques. Numerical simulations employing the Adams-Moulton scheme illustrate the influence of memory-dependent dynamics,revealing that lower fractional orders slow the spread of infection by regulating bacterial growth and host-pathogen interactions. These results underscore the utility of fractional-order modeling in epidemiology, suggesting that incorporating memory effects enhances the predictive capability of disease models. Future research should focus on integrating optimal control strategies to mitigate cholera outbreaks effectively.

Keywords: Fractional Order, Stability, Optimal Control, Basic reproduction number, Vibrio Cholera.

1 Introduction

Cholera is an acute diarrheal disease transmitted through contaminated water, caused by the gram-negative bacterium Vibrio cholerae,which mainly inhabits aquatic environments and affects the small intestine [1]. As the primary cause of cholera, Vibrio cholerae results in severe diarrhea, primarily impacting populations in developing countries[2].The disease spreads through direct contact with contaminated water or seafood, as well as through human-to-human transmission of the bacterium[3].Cholera symptoms include the sudden onset of high fever,significant weight loss, nausea, vomiting, irregular heartbeat, and dehydration caused by severe fluid loss [4]. Considering the transmission mechanisms of cholera is essential for developing effective prevention and control strategies, as the disease is often worsened by seasonal bacterial blooms, poor sanitation, and contaminated water sources [5].
Cholera represents a major global public health threat, with estimates indicating that 1.3 to 1.4 million people are infected each year, leading to around 21,000 to 43,000 deaths globally [6]. The quick onset of the disease can cause intense vomiting and diarrhea, which raises the risk of severe dehydration.
Mathematical models in epidemiology offer crucial insights into how diseases spread and help guide the development of effective containment strategies.The idea of using mathematical models to understand the transmission of endemic diseases can be traced back to Daniel Bernoulli's 1766 study on smallpox [7].In 1927, Kermack and McKendrick made foundational contributions that established the use of systems of differential equations to understand disease transmission [8].Since then,numerous studies have employed mathematical modeling to analyze and predict cholera outbreaks,thereby improving public health decision-making [9]. Recent developments in fractional calculus have led to the introduction of fractional derivatives and integrals, which exhibit non-local characteristics, making them especially effective for modeling biological systems [10,11,12].For example,studies have integrated memory effects into conventional models,like the SIR model,to more accurately represent disease transmission dynamics[11].Other research has investigated fractional differential models across different biological contexts,showcasing their effectiveness in

* Corresponding author e-mail: tululeta2008@gmail.com

representing complex systems[13]. The Atangana-Baleanu fractional derivative,in particular, has proven valuable in studying natural phenomena by connecting the current state with all past states [14].This approach offers increased flexibility in modeling by allowing the selection of any real number for the derivative order,which improves system stability and provides extra parameters for numerical simulations [15]. The increasing interest in fractional-order differential equations (FDEs) highlights their importance in modeling real-world systems with memory [16]. Recent applications cover a variety of infectious diseases, such as tuberculosis and COVID-19, demonstrating the versatility of fractional models in epidemiology [17].

For example, Leo [18] advanced an ML reference cholera model that can be used to overcome the existing complexities of modeling the illness. His results shows, at an average of 87%,that the developed measures can mitigate a large number of datasets,including environmental factors,for the timely prediction of cholera epidemics in Tanzania. In [19],a mathematical model for cholera considering vaccination output grow to be proposed. In [20],Capasso and Paveri-Fontana deduced a mathematical model for the 1973 cholera epidemic withinside the European Mediterranean region.In 2017, the transmission dynamics of cholera in Yemen were investigated thru Nishiura et al [21].Lastly, a model containing optimal intervention strategies for cholera control was formulated in [22]. Luchko and Yamamoto [23] explored a new differential operator with a substantial kernel function. Due to the existence of flexibility in choosing the kernel, they provide a basis for a broad range of applications [24].Changing the kernel in the general derivative leads to the investigate of various asymptotic behaviors. Mukandavire et al explored a model with saturation effect to assess the reproduction number of cholera outbreak in Zimbabwe from 2008 to 2009 [25].In 2011, Jin Wang and Chairat Modnak elongate Mukandavire et al. model to cognizance at the consequences of vaccination, restoration treatment, and water sanitation at the cholera outbreaks [26]. In 2016,Lemos-Paiao et al considered SIQRB cholera model to decrease the number of infected individuals via treatment through quarantine [27].However,traditional integer-order models often lack the flexibility to improve stability zones,as they are inherently local in nature.

Building upon the preceding discussion, this study introduces an innovative mathematical model that employs the general form of the Atangana-Baleanu fractional derivative to represent the dynamics of a cholera outbreak.To the best of our knowledge,this is the first analysis applying such a fractional derivative form to cholera,thereby enhancing the model's flexibility through the use of various kernels and fractional orders to capture the complex behaviors of the biological system under study. Furthermore,the SAIQR-B endemic model incorporating the Atangana-Baleanu fractional derivative has not been previously explored.By leveraging these considerations, we propose a fractional order mathematical model for cholera transmission dynamics focusing on the Susceptible- Asymptomatic- Infected-Quarantined-Recovered and Bacterium(SAIQR-B)compartments.This represents the inaugural application of the Atangana-Baleanu fractional derivative within the SAIQR-B model framework.

The remainder of this paper is structured as follows: Section 2 presents the model description and formulation; Section 3 establishes the existence and uniqueness of solutions,including positivity and boundedness within the context of the Atangana-Baleanu fractional operator;Section 4 presents the model analysis; Section 5 details the numerical solutions and simulations of the SAIQR-B model; and Section 6 concludes the study.

2 Cholera Model Description and Formulation

The model separated the entire population into five groups, each of which included vulnerable people. $S(t)$ are those people who are healthy now but may have the illness in the future, asymptomatic individuals $A(t)$, individuals who are already cholera infected but has no cholera symptoms, symptomatic individuals $I(t)$, are individuals who are already cholera infected and shows cholera disease symptoms, quarantined individuals $Q(t)$, are individuals who are infectious and compulsory quarantined to get treatment based on the patients clinical results, and recovered individuals $R(t)$, are individuals who are recovered from Cholera disease by treatment at a time. Moreover, $B(t)$, is the concentration of Vibro Cholerae bacterium in an aquatic environment is tracked as an additional compartment.

The model also assumed that the human population recruited to susceptible compartment at a rate Π and the concentration of the environmental bacteria is described by a logistic growth model with the intrinsic growth rate r and the carrying capacity K [21]. Infectious individuals like asymptomatic, symptomatic and quarantined individuals contribute to the bacteria population in the environment at rate δ_1,δ_2 and δ_3 respectively, and μ_B is the bacteria removal rate due to water sanitation. Susceptible individuals may become infected by Cholera infection either directly through human to human transmission at a force of infection $\lambda_1 = (\frac{\beta_1(I+qA)}{N})$, where β_1 is the effective contact rate and q is the transmission coefficient for asymptomatic individuals or indirectly from environment to human by ingestion of contaminated water by Vibrio Cholerae bacterium at a rate $\lambda_2 = \frac{\beta_2 B}{k+B}$, where k is the concentration of Vibrios in contaminated water in the environment, and β_2 ingestion rate. Susceptible individuals progress to asymptomatic compartment with probability $(1-p)$, and to the symptomatic compartment with probability p. The quarantined compartment increases with individuals who come from asymptomatic and symptomatic compartments with a rate ϕ and ω respectively. Then quarantined individuals

are recovered as a result of cholera treatment at a rate θ. The recovered individuals who lose immunity become susceptible at a rate α. In all compartments, μ is the natural death rate of individuals, but in the infectious compartment ξ is Cholera disease induced death rate. All parameters in the model are non-negative. The schematic diagram of Cholera model is shown in Fig.1.

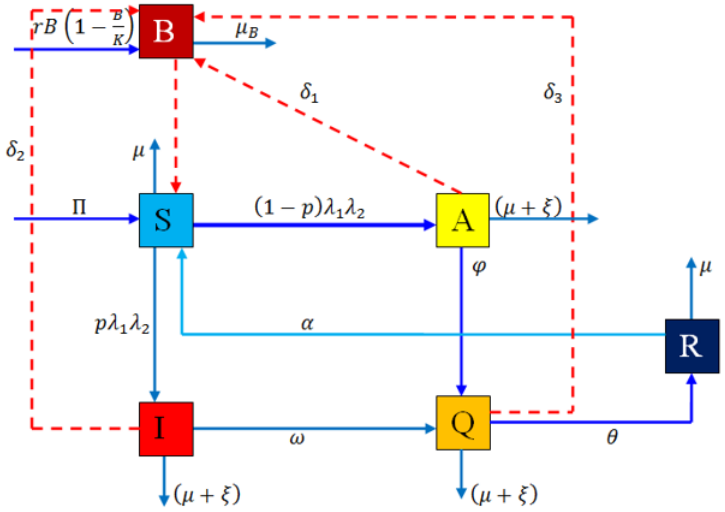

Fig. 1: Schematic Diagram of Cholera Model

Based on the aforementioned model assumption with the description and schematic diagram we obtain the following version of equations.

$$\begin{cases} \frac{dS}{dt} = \Pi - \lambda_1\lambda_2 S - \mu S + \alpha R, \\ \frac{dA}{dt} = (1-p)\lambda_1\lambda_2 S - (\varphi + \delta_1 + \mu + \xi)A, \\ \frac{dI}{dt} = p\lambda_1\lambda_2 S - (\omega + \delta_2 + \mu + \xi)I, \\ \frac{dQ}{dt} = \varphi A + \omega I - (\theta + \delta_3 + \mu + \xi)Q, \\ \frac{dR}{dt} = \theta Q - (\mu + \alpha)R, \\ \frac{dB}{dt} = rB(1-\frac{B}{K}) + \delta_1 A + \delta_2 I + \delta_3 Q - \mu_B B. \end{cases} \tag{1}$$

With initial condition $S(0) > 0, A(t) \geq 0, I(t) \geq 0, Q(t) \geq 0, R(t) \geq 0$, and $B(t) \geq 0$.
However, the classical model (1) does not include memory effects due to the existence of integer-order derivatives in the Dynamics. To overcome this issue, here we modify the model (1) by replacing the ordinary time-derivative with Atangana-Baleanu fractional derivative. Following these considerations, the new fractional model for the cholera dynamics is as the following system.

$$\begin{cases} {}^{ABC}_{0}D^{\sigma}_{t} S(t) = F_1(t,S), \\ {}^{ABC}_{0}D^{\sigma}_{t} A(t) = F_2(t,A), \\ {}^{ABC}_{0}D^{\sigma}_{t} I(t) = F_3(t,I), \\ {}^{ABC}_{0}D^{\sigma}_{t} Q(t) = F_4(t,Q), \\ {}^{ABC}_{0}D^{\sigma}_{t} R(t) = F_5(t,R), \\ {}^{C}_{0}D^{\sigma}_{t} B(t) = F_6(t,B). \end{cases} \tag{2}$$

where the kernels are given by

$$\begin{cases} F_1(t,S) = \Pi - \lambda_1\lambda_2 S - \mu S + \alpha R, \\ = F_2(t,A) = (1-p)\lambda_1\lambda_2 S - (\varphi + \delta_1 + \mu + \xi)A, \\ F_3(t,I) = P\lambda_1\lambda_2 S - (\omega + \delta_2 + \mu + \xi)I, \\ F_4(t,Q) = \varphi A + \omega I - (\theta + \delta_3 + \mu + \xi)Q, \\ F_5(t,R) = \theta Q - (\mu + \alpha)R, \\ F_6(t,B) = rB(1 - \frac{B}{K}) + \delta_1 A + \delta_2 I + \delta_3 Q - \mu_B B. \end{cases} \tag{3}$$

With initial condition $S(0) = S_0, A(0) = A_0, I(0) = I_0, Q(0) = Q_0, R(0) = R_0, B(0) = B_0$. and $\lambda_1 = (\frac{\beta_1(I+qA)}{N})$, $\lambda_2 = \frac{\beta_2 B}{k+B}$ where all the parameters are assumed to be non-negative, and ${}_0^{ABC}D_t^{\sigma}$ denotes the Atangana-Baleanu fractional derivative of order $\sigma \in (0,1]$ for function $f(t)$ such that [9].

Preliminaries

In this section, we overview numerous key definitions, lemmas, and ideas which can be essential to apprehend our suggested.

Definition 1.*([29,31]). Let $f \in C^1(a,b)$, $a < b$,be a function, and $\sigma \in [0,1]$. The Atangana-Baleanu (AB) fractional derivative in Caputo type of order σ is given by*

$${}_a^{ABC}D_t^{\sigma} f(t) = \frac{G(\sigma)}{1-\sigma}\int_a^t \frac{df}{dk} E_{\sigma}[-\frac{\sigma}{1-\sigma}(t-k)^{\sigma}]dk, \tag{4}$$

where $G(\sigma)$ is the normalization function given by $G(\sigma) = 1 - \sigma + \frac{\sigma}{\Gamma(\sigma)}$, characterized by $G(0) = G(1) = 1$, and the Mittag-Leffler function $E_{\sigma(z)}$ with $\mathbf{C}$ the set of the complex number is given by
$E_{\sigma(z)} \sum_{\beta=0}^{\infty} \frac{z^{\beta}}{\Gamma(1+\sigma\beta)}, \sigma, z \in \mathbf{C}, \mathbf{R}(\sigma) > 0.$

Definition 2.*The AB fractional integral of the function $f \in C^1(a,b)$ is given by [20,21,22]*

$${}_a^{AB}I_t^{\sigma} f(t) = \frac{1-\sigma}{G(\sigma)} + \frac{\sigma}{G(\sigma)\Gamma(\sigma)}\int_a^t f(k)(t-k)^{\sigma-1}dk. \tag{5}$$

Lemma 1.*([24]) The AB fractional derivative and AB fractional integral of the function $f \in C^1(a,b)$ satisfies the Newton-Leibniz equality*
${}_a^{AB}I_t^{\sigma}({}_a^{ABC}D_t^{\sigma} f(t)) = f(t) - f(a).$

Lemma 2.*([25,26]) For two functions $f, g \in \Delta^1(a,b), b > a$, the AB fractional derivative satisfies the following inequality:*
$\|{}_a^{ABC} D_t^{\sigma} f(t) - {}_a^{ABC} D_t^{\sigma} g(t) \| \leq \Delta \| f(t) - g(t) \|.$

3 Basic Properties of Model

3.1 Invariant Region

In the subsequent analyses, we will show that the version plays well-posed in each epidemiologically and mathematically. The boundedness of the solutions are performed in two parts: the human population and bacterial population. For the human population, the first five equations of system (2) are summed to give

$${}_0^{ABC}D_t^{\sigma} N(t) = \Pi - \mu N(t) - I\alpha_1 - A(\delta_1 + \xi) - I(\delta_2 + \xi) - Q(\delta_3 + \xi) \leq \Pi - \mu N(t). \tag{6}$$

Applying the Laplace transform of the above inequality, we have

$$\lambda^{\sigma}\mathscr{L}[N(t)]-\lambda^{\sigma-1}N(0)\leq\frac{\Pi}{\lambda}-\mu\mathscr{L}[N(t)], \tag{7}$$

that can be written as

$$\mathscr{L}[N(t)]\leq\frac{\lambda^{-1}}{\lambda^{\sigma}+\mu}\Pi+\frac{\lambda^{\sigma-1}}{\lambda^{\sigma}+\mu}N(0), \tag{8}$$

applying the inverse of the Laplace transform on inequality (6) gives

$$N(t)\leq\Pi t^{\sigma}E_{\sigma,\sigma+1}(-\mu t^{\sigma})+E_{\sigma,1}(-\mu t^{\sigma})N(0)=(-\frac{\Pi}{\mu}+N(0))E_{\sigma,1}(-\mu t^{\sigma})+\frac{\Pi}{\mu}, \tag{9}$$

where

$$E_{a,b}(z)=\sum_{k=0}^{\infty}\frac{z^k}{\Gamma(ak+b)}$$

is Mittag-Leffler function with parameters a and b. It is clear that $N(0)\leq\frac{\Pi}{\mu}$ when $t=0$. Then, $N(t)\leq\frac{\Pi}{\mu}$ can be derived from $E_{\sigma,1}(-\mu t^{(}\sigma))\geq 0$.
Next, for the bacterial population, it follows that

$${}_0^{ABC}D_t^{\sigma}B(t)\leq rB(1-\frac{B}{K})+\delta_1 A+\delta_2 I+\delta_2 Q-\mu_B B, \tag{10}$$

thus, one has

$$B(t)\leq\frac{(\delta_1+\delta_2+\delta_3)}{\mu\mu_B r}\Pi K.$$

As such, the feasible region for system (2) is given by

$$\Omega=\left\{(S,A,I,Q,R,B)\in R_+^6:0\leq N(t)\leq\frac{\Pi}{\mu},B(t)\leq\frac{(\delta_1+\delta_2+\delta_3)}{\mu\mu_B r}\Pi K\right\}. \tag{11}$$

3.2 Positivity of Solutions

Theorem 1.*For the given initial conditions , the solutions of system (2) are positive and bounded for all $t\geq 0$.*

*Proof.*One of the important characteristics of epidemiological models is that their solutions are both positive and bounded. In order to ensure this, we establish that all of the state variables are non-negative for any time $n>0$, which implies that a trajectory starting with a positive initial condition will stay positive for all $n>0$. Thus, system (2) gives

$$\begin{cases}{}_0^{ABC}D_t^{\sigma}S(t)|S=0=\Pi+\alpha R\geq 0,\\ {}_0^{ABC}D_t^{\sigma}A(t)|A=0=(1-p)\lambda_1\lambda_2 S\geq 0,\\ {}_0^{ABC}D_t^{\sigma}I(t)|I=0==p\lambda_1\lambda_2 I\geq 0,\\ {}_0^{ABC}D_t^{\sigma}Q(t)|Q=0=\varphi A+\omega I\geq 0,\\ {}_0^{ABC}D_t^{\sigma}R(t)|R=0=\theta Q\geq 0,\\ {}_0^{ABC}D_t^{\sigma}B(t)|B=0=\delta_1 A+\delta_2 I+\delta_2 Q\geq 0.\end{cases} \tag{12}$$

Based on analysis and discussion described above, the solutions of the system (2) remain positive and bounded.

3.3 Existence and Uniqueness of the Solutions

In this section, existence and uniqueness of the fractional-order model (2) is deliberated. To show the existence of the solution to model (2), we use the famous theorem referred to as the Banach fixed point theorem. For an extensive study on fixed points and contractions, we refer the reader to [42] and the references therein. To show the existence and uniqueness Of the solution, we continue as follows. Applying the AB fractional integral to model (2), we obtain

$$\begin{cases} S(t)-S(0)=\frac{1-\sigma}{G(\sigma)}F_1(t,S)+\frac{\sigma}{G(\sigma)\Gamma(\sigma)}\int_0^t F_1(k,S)(t-k)^{\sigma-1}dk, \\ A(t)-A(0)=\frac{1-\sigma}{G(\sigma)}F_2(t,S)+\frac{\sigma}{G(\sigma)\Gamma(\sigma)}\int_0^t F_2(k,A)(t-k)^{\sigma-1}dk, \\ I(t)-I(0)=\frac{1-\sigma}{G(\sigma)}F_3(t,S)+\frac{\sigma}{G(\sigma)\Gamma(\sigma)}\int_0^t F_3(k,I)(t-k)^{\sigma-1}dk, \\ Q(t)-Q(0)=\frac{1-\sigma}{G(\sigma)}F_4(t,S)+\frac{\sigma}{G(\sigma)\Gamma(\sigma)}\int_0^t F_4(k,Q)(t-k)^{\sigma-1}dk, \\ R(t)-R(0)=\frac{1-\sigma}{G(\sigma)}F_5(t,S)+\frac{\sigma}{G(\sigma)\Gamma(\sigma)}\int_0^t F_5(k,R)(t-k)^{\sigma-1}dk, \\ B(t)-B(0)=\frac{1-\sigma}{G(\sigma)}F_6(t,S)+\frac{\sigma}{G(\sigma)\Gamma(\sigma)}\int_0^t F_6(k,B)(t-k)^{\sigma-1}dk, \end{cases} \tag{13}$$

Consider the set $C=D(J)\times D(J)\times D(J)\times D(J)\times D(J)$ where $D(J)=C[0,T]$ is the Banach space of real-valued continuous functions defined on an interval $J=[0,T]$ with the corresponding norm defined by $\|(S,A,I,Q,R,B)\|=\|S\|+\|A\|+\|I\|+\|Q\|+\|R\|+\|B\|$, where
$\|S\|=Sup_{t\in J}|S(t)|,\|A\|=Sup_{t\in J}|A(t)|,\|I\|=Sup_{t\in J}|I(t)|,\|Q\|=Sup_{t\in J}|Q(t)|,\|R\|=Sup_{t\in J}|R(t)|,\|B\|=Sup_{t\in J}|B(t)|$.

Theorem 2.*(Lipschitz condition and contraction) For each of the kernels F_1,F_2,F_3,F_4,F_5,F_6 in (2), there exists $M_i>0, i=1,2,3,4,5,6$ such that*

$$\begin{cases} \|F_1(t,S)-F_1(t,S_1)\|\leq M_1\|S(t)-S_1(t)\|, \\ \|F_2(t,A)-F_2(t,A_1)\|\leq M_2\|A(t)-A_1(t)\|, \\ \|F_3(t,I)-F_3(t,I_1)\|\leq M_3\|I(t)-I_1(t)\|, \\ \|F_4(t,Q)-F_4(t,Q_1)\|\leq M_4\|Q(t)-Q_1(t)\|, \\ \|F_5(t,R)-F_5(t,R_1)\|\leq M_5\|R(t)-R_1(t)\|, \\ \|F_6(t,B)-F_6(t,B_1)\|\leq M_6\|B(t)-B_1(t)\|. \end{cases}$$

and are contractions for $0\leq M_i<1, i=1,2,3,4,5,6$.

Proof.
$$\begin{aligned} \|F_1(t,S)-F_1(t,S_1)\| &= \|(\Pi-\lambda_1\lambda_2 S-\mu S+\alpha R)-(\Pi-\lambda_1\lambda_2 S_1-\mu S_1+\alpha R)\| \\ &= \|(-\lambda_1\lambda_2 S-\mu S+\lambda_1\lambda_2 S_1+\mu S_1)\| \\ &== \|\lambda_1\lambda_2(S_1-S)+\mu(S_1-S)\| \\ &\leq (\lambda_1\lambda_2+\mu)\|(S_1-S)\| \\ &\leq M_1\|(S_1-S)\|, \end{aligned}$$

where $M_1=\lambda_1\lambda_2+\mu$,
It then follows that $F_1(t,S)$ satisfies the Lipschitz condition with Lipschitz constant $M_1=\lambda_1\lambda_2+\mu$. Moreover, if $0\leq M_1<1$, then $F_1(t,S)$ is a contraction. Again for second

$$\begin{aligned} \|F_2(t,S)-F_2(t,A_1)\| &= \|((1-p)\lambda_1\lambda_2 S-(\varphi+\delta_1+\mu+\xi)A)-((1-p)\lambda_1\lambda_2 S-(\varphi+\delta_1+\mu+\xi)A_1)\| \\ &= \|-(\varphi+\delta_1+\mu+\xi)A)+(\varphi+\delta_1+\mu+\xi)A_1)\| \\ &= (\varphi+\delta_1+\mu+\xi)\|(A_1-A)\| \\ &\leq (\varphi+\delta_1+\mu+\xi)\|(A_1-A)\| \\ M_2 &\leq \|(A_1-A)\|, \end{aligned}$$

where $M_2=\varphi+\delta_1+\mu+\xi$,
It then follows that $F_2(t,A)$ satisfies the Lipschitz condition with Lipschitz constant $M_2=\varphi+\delta_1+\mu+\xi$. Moreover, if $0\leq M_2<1$, then $F_2(t,A)$ is a contraction.
Similarly, we can show the existence of $M_i, i=3,4,5,6$, and a contraction principle for $F_3(t,I),F_4(t,Q),F_5(t,R),F_6(t,B)$,

$0 \leq M_i < 1$. Now for $= t_n, n = 1,23,4,5,6$, define the following recursive form of (13)

$$\begin{cases} S_n(t) = \frac{1-\sigma}{G(\sigma)} F_1(t, S_{n-1}) + \frac{\sigma}{G(\sigma)\Gamma(\sigma)} \int_0^t F_1(k, S_{n-1})(t-k)^{\sigma-1} dk, \\ A_n(t) = \frac{1-\sigma}{G(\sigma)} F_2(t, A_{n-1}) + \frac{\sigma}{G(\sigma)\Gamma(\sigma)} \int_0^t F_2(k, An-1)(t-k)^{\sigma-1} dk, \\ I_n(t) = \frac{1-\sigma}{G(\sigma)} F_3(t, I_{n-1}) + \frac{\sigma}{G(\sigma)\Gamma(\sigma)} \int_0^t F_3(k, I_{n-1})(t-k)^{\sigma-1} dk, \\ Q_n(t) = \frac{1-\sigma}{G(\sigma)} F_4(t, Q_{n-1}) + \frac{\sigma}{G(\sigma)\Gamma(\sigma)} \int_0^t F_4(k, Q_{n-1})(t-k)^{\sigma-1} dk, \\ R_n(t) = \frac{1-\sigma}{G(\sigma)} F_5(t, R_{n-1}) + \frac{\sigma}{G(\sigma)\Gamma(\sigma)} \int_0^t F_5(k, R_{n-1})(t-k)^{\sigma-1} dk, \\ B_n(t) = \frac{1-\sigma}{G(\sigma)} F_6(t, B_{n-1}) + \frac{\sigma}{G(\sigma)\Gamma(\sigma)} \int_0^t F_6(k, S_{n-1})(t-k)^{\sigma-1} dk, \end{cases} \tag{14}$$

with initial conditions $S_0(t)S(0), A_0(t) = A(0), I_0(t) = I(0), Q_0(t) = Q(0), R_0(t) = R(0), B_0(t) = B(0)$.The differences between successive terms in (14) are expressed as follows;

$$\begin{cases} B_{1n}(t) = S_n(t) - S_{n-1}(t) \\ = \frac{1-\sigma}{G(\sigma)} (F_1(t, S_{n-1}) - F_1(t, S_{n-2})) \\ + \frac{\sigma}{G(\sigma)\Gamma(\sigma)} \int_0^t (F_1(t, S_{n-1}) - F_1(t, S_{n-2}))(t-k)^{\sigma-1} dk, \\ B_{2n}(t) = A_n(t) - A_{n-1}(t) \\ = \frac{1-\sigma}{G(\sigma)} (F_2(t, A_{n-1}) - F_2(t, A_{n-2})) \\ + \frac{\sigma}{G(\sigma)\Gamma(\sigma)} \int_0^t (F_2(t, A_{n-1}) - F_2(t, A_{n-2}))(t-k)^{\sigma-1} dk, \\ B_{3n}(t) = I_n(t) - I_{n-1}(t) \\ = \frac{1-\sigma}{G(\sigma)} (F_3(t, I_{n-1}) - F_3(t, I_{n-2})) \\ + \frac{\sigma}{G(\sigma)\Gamma(\sigma)} \int_0^t (F_3(t, I_{n-1}) - F_3(t, I_{n-2}))(t-k)^{\sigma-1} dk, \\ B_{4n}(t) = Q_n(t) - Q_{n-1}(t) \\ = \frac{1-\sigma}{G(\sigma)} (F_4(t, Q_{n-1}) - F_4(t, Q_{n-2})) \\ + \frac{\sigma}{G(\sigma)\Gamma(\sigma)} \int_0^t (F_4(t, Q_{n-1}) - F_4(t, Q_{n-2}))(t-k)^{\sigma-1} dk, \\ B_{5n}(t) = R_n(t) - R_{n-1}(t) \\ = \frac{1-\sigma}{G(\sigma)} (F_5(t, R_{n-1}) - F_5(t, R_{n-2})) \\ + \frac{\sigma}{G(\sigma)\Gamma(\sigma)} \int_0^t (F_5(t, R_{n-1}) - F_5(t, R_{n-2}))(t-k)^{\sigma-1} dk, \\ B_{6n}(t) = B_n(t) - B_{n-1}(t) \\ = \frac{1-\sigma}{G(\sigma)} (F_6(t, B_{n-1}) - F_6(t, B_{n-2})) \\ + \frac{\sigma}{G(\sigma)\Gamma(\sigma)} \int_0^t (F_6(t, B_{n-1}) - F_6(t, B_{n-2}))(t-k)^{\sigma-1} dk. \end{cases} \tag{15}$$

Taking the norm on both sides of each equation in (13), we have

$$\begin{cases} \| B_{1n}(t) \| = \| S_n(t) - S_{n-1}(t) \| \\ = \frac{1-\sigma}{G(\sigma)} \| (F_1(t,S_{n-1}) - F_1(t,S_{n-2})) \| \\ + \frac{\sigma}{G(\sigma)\Gamma(\sigma)} \int_0^t \| (F_1(t,S_{n-1}) - F_1(t,S_{n-2})) \| (t-k)^{\sigma-1} dk, \\ \| B_{2n}(t) \| = \| A_n(t) - A_{n-1}(t) \| \\ = \frac{1-\sigma}{G(\sigma)} \| (F_2(t,A_{n-1}) - F_2(t,A_{n-2})) \| \\ + \frac{\sigma}{G(\sigma)\Gamma(\sigma)} \int_0^t \| (F_2(t,A_{n-1}) - F_2(t,A_{n-2})) \| (t-k)^{\sigma-1} dk, \\ \| B_{3n}(t) \| = \| I_n(t) - I_{n-1}(t) \| \\ = \frac{1-\sigma}{G(\sigma)} \| (F_3(t,I_{n-1}) - F_3(t,I_{n-2})) \| \\ + \frac{\sigma}{G(\sigma)\Gamma(\sigma)} \int_0^t \| (F_3(t,I_{n-1}) - F_3(t,I_{n-2})) \| (t-k)^{\sigma-1} dk, \\ \| B_{4n}(t) \| = \| Q_n(t) - Q_{n-1}(t) \| \\ = \frac{1-\sigma}{G(\sigma)} \| (F_4(t,Q_{n-1}) - F_4(t,Q_{n-2})) \| \\ + \frac{\sigma}{G(\sigma)\Gamma(\sigma)} \int_0^t \| (F_4(t,Q_{n-1}) - F_4(t,Q_{n-2})) \| (t-k)^{\sigma-1} dk, \\ \| B_{5n}(t) \| = \| R_n(t) - R_{n-1}(t) \| \\ = \frac{1-\sigma}{G(\sigma)} \| (F_5(t,R_{n-1}) - F_5(t,R_{n-2})) \| \\ + \frac{\sigma}{G(\sigma)\Gamma(\sigma)} \int_0^t \| (F_5(t,R_{n-1}) - F_5(t,R_{n-2})) \| (t-k)^{\sigma-1} dk, \\ \| B_{6n}(t) \| = \| B_n(t) - B_{n-1}(t) \| \\ = \frac{1-\sigma}{G(\sigma)} \| (F_6(t,B_{n-1}) - F_6(t,B_{n-2})) \| \\ + \frac{\sigma}{G(\sigma)\Gamma(\sigma)} \int_0^t \| (F_6(t,B_{n-1}) - F_6(t,B_{n-2})) \| (t-k)^{\sigma-1} dk. \end{cases} \tag{16}$$

Furthermore, the first equality in (16) can be reduced to the following expressions;
$\| B_{1n}(t) \| \| S_n(t) - S_{n-1}(t) \|$
$\leq \frac{1-\sigma}{G(\sigma)} \| (F_1(t,S_{n-1}) - F_1(t,S_{n-2})) \|$
$+ \frac{\sigma}{G(\sigma)\Gamma(\sigma)} \int_0^t \| (F_1(t,S_{n-1}) - F_1(t,S_{n-2})) \| (t-k)^{\sigma-1} dk$
$\leq \frac{1-\sigma}{G(\sigma)} M_1 \| S_{n-1} - S_{n-2} \| + \frac{\sigma}{G(\sigma)\Gamma(\sigma)} M_1 \int_0^t \| S_{n-1}) - S_{n-2} \| (t-k)^{\sigma-1} dk$
$\leq M_1 \| B_{1(n-1)}(t) \| | \frac{1-\sigma}{G(\sigma)} + \frac{\sigma}{G(\sigma)\Gamma(\sigma)} |.$
As a result, we have

$$\| B_{1n}(t) \leq M_1 \| | \frac{1-\sigma}{G(\sigma)} + \frac{\sigma}{G(\sigma)\Gamma(\sigma)} | \| B_{1(n-1)}(t) \|, \tag{17}$$

Similarly, the remaining expressions of (17) can be reduced to the following expressions:

$$\begin{cases} \| B_{2n}(t) \leq M_2 \| | \frac{1-\sigma}{G(\sigma)} + \frac{\sigma}{G(\sigma)\Gamma(\sigma)} | \| B_{2(n-1)}(t) \|, \\ \| B_{3n}(t) \leq M_3 \| | \frac{1-\sigma}{G(\sigma)} + \frac{\sigma}{G(\sigma)\Gamma(\sigma)} | \| B_{3(n-1)}(t) \|, \\ \| B_{4n}(t) \leq M_4 \| | \frac{1-\sigma}{G(\sigma)} + \frac{\sigma}{G(\sigma)\Gamma(\sigma)} | \| B_{4(n-1)}(t) \|, \\ \| B_{5n}(t) \leq M_5 \| | \frac{1-\sigma}{G(\sigma)} + \frac{\sigma}{G(\sigma)\Gamma(\sigma)} | \| B_{5(n-1)}(t) \|, \\ \| B_{6n}(t) \leq M_6 \| | \frac{1-\sigma}{G(\sigma)} + \frac{\sigma}{G(\sigma)\Gamma(\sigma)} | \| B_{16(n-1)}(t) \| . \end{cases} \tag{18}$$

Theorem 3. *The AB fractional model given in (2) has a solution if we can find Z_0 satisfying the inequality*

$$(\frac{1-\sigma}{G(\sigma)} + \frac{Z_0^{\sigma}}{G(\sigma)\Gamma(\sigma)}) M_i < 1, i = 1,2,3,4,5,6. \tag{19}$$

*Proof.*From (15) and (16) we have

$$\begin{cases} \| B_{1n}(t) \| \leq \| S(0) \| [(\frac{1-\sigma}{G(\sigma)} + \frac{Z_0^\sigma}{G(\sigma)\Gamma(\sigma)})M_1]^n, \\ \| B_{2n}(t) \| \leq \| A(0) \| [(\frac{1-\sigma}{G(\sigma)} + \frac{Z_0^\sigma}{G(\sigma)\Gamma(\sigma)})M_2]^n, \\ \| B_{3n}(t) \| \leq \| I(0) \| [(\frac{1-\sigma}{G(\sigma)} + \frac{Z_0^\sigma}{G(\sigma)\Gamma(\sigma)})M_3]^n, \\ \| B_{4n}(t) \| \leq \| Q(0) \| [(\frac{1-\sigma}{G(\sigma)} + \frac{Z_0^\sigma}{G(\sigma)\Gamma(\sigma)})M_4]^n, \\ \| B_{5n}(t) \| \leq \| R(0) \| [(\frac{1-\sigma}{G(\sigma)} + \frac{Z_0^\sigma}{G(\sigma)\Gamma(\sigma)})M_5]^n, \\ \| B_{6n}(t) \| \leq \| B(0) \| [(\frac{1-\sigma}{G(\sigma)} + \frac{Z_0^\sigma}{G(\sigma)\Gamma(\sigma)})M_6]^n. \end{cases} \tag{20}$$

The existence of the solution (the existence of a fixed point) is confirmed by Theorem 2, and we have to show that the functions $S(t), A(t), I(t), Q(t), R(t), B(t)$ are solutions of model (2).
Let us assume that the following are satisfied:

$$\begin{cases} S(t) - S(0) = S_n(t) - b_{1n}(t), \\ A(t) - A(0) = A_n(t) - b_{2n}(t), \\ I(t) - I(0) = I_n(t) - b_{3n}(t), \\ Q(t) - Q(0) = Q_n(t) - b_{4n}(t), \\ R(t) - R(0) = R_n(t) - b_{5n}(t), \\ B(t) - B(0) = B_n(t) - b_{6n}(t). \end{cases} \tag{21}$$

From (19) we obtain
$\| b_{1n}(t) \| \leq \frac{1-\sigma}{G(\sigma)} \| (F_1(\gamma, S_n) - F_1(\gamma, S_{n-1})) \|$
$+ \frac{\sigma}{G(\sigma)\Gamma(\sigma)} \int_0^t \| (F_1(\gamma, S_n) - F_1(\gamma, S_{n-1})) \| (\gamma - k)^{\sigma-1} dk,$
$\leq \frac{1-\sigma}{G(\sigma)} M_1 \| S_n - S_{n-1} \| + \frac{\sigma^n}{G(\sigma)\Gamma(\sigma)} \| S_n - S_{n-1} \|.$
Repeating the process recursively leads to
$\| b_{1n}(t) \| \leq [1 - \sigma G(\sigma) + \frac{t^\sigma}{G(\sigma)\Gamma(\sigma)}]^{n+1} M_1^n \| S_n - S_{n-1} \|^n$
which at $t = Z_0^\sigma$ yields

$$\| b_{1n}(t) \| \leq [1 - \sigma G(\sigma) + \frac{Z_0^\sigma}{G(\sigma)\Gamma(\sigma)}]^{n+1} M_1^n \| S_n - S_{n-1} \|^n, \ \| b_{1n}(t) \| \text{ß} 0. \tag{22}$$

Applying the limit to both sides of (20) as nß∞, we see that $\| b_{1n}(t) \|$ ß0 for
$(\frac{1-\sigma}{G(\sigma)} + \frac{Z_0^\sigma}{G(\sigma)\Gamma(\sigma)})M_1 < 1.$
Similarly, we can show that $\| b_{2n}(t) \|$ ß0, $\| b_{3n}(t) \|$ ß0, $\| b_{4n}(t) \|$ ß0, $\| b_{5n}(t) \|$ ß0, $\| b_{6n}(t) \|$ ß0,
$(\frac{1-\sigma}{G(\sigma)} + \frac{t^\sigma}{G(\sigma)\Gamma(\sigma)})M_i < 1, i = 2,3,4,5,6.$

Theorems 2 and 3 guarantee the existence of the solution of model (2) by the Banach fixed point theorem. The uniqueness of the solution is proved in Theorem 4

Theorem 4.*(Uniqueness of solution) The AB fractional model (2) has a unique solution, provided that*

$$(\frac{1-\sigma}{G(\sigma)} + \frac{t^\sigma}{G(\sigma)\Gamma(\sigma)})M_i < 1, i = 2,3,4,5,6. \tag{23}$$

*Proof.*Let us assume that $S_1(t), A_1(t), I_1(t), Q_1(t), R_1(t), B_1(t)$ are also solutions to (2). Then
$S_n(t) - S_{n-1}(t) = \frac{1-\sigma}{G(\sigma)}(F_1(t, S_{n-1}) - F_1(t, S_{n-2})) + \frac{\sigma}{G(\sigma)\Gamma(\sigma)} \int_0^t (F_1(t, S_{n-1}) - F_1(t, S_{n-2}))(t-k)^{\sigma-1} dk.$
Taking the norm of both sides, we obtain
$\| St - S_1(t) \| \leq \frac{1-\sigma}{G(\sigma)} M_1 \| S - S_1 \| + \frac{t^\sigma}{G(\sigma)\Gamma(\sigma)} M_1 \| S - S_1 \|.$
Since $(1 - (\frac{1-\sigma}{G(\sigma)} + \frac{t^\sigma}{G(\sigma)\Gamma(\sigma)})) > 0$, we obtain $\| St - S_1(t) \| = 0$. Thus we have $S(t) = S_1(t)$.
Similarly, we can show that $A(t) = A_1(t), I(t) = I_1(t), Q(t) = Q_1(t), R(t) = R_1(t), B(t) = B_1(t)$, which completes the proof of Theorem 4.

4 Cholera Model Analysis

4.1 Cholera Disease Free Equilibrium Point

A cholera-free equilibrium $E_0 = (S_0, A_0, I_0, Q_0, R_0, B_0)$ of cholera model is a point where cholera infection is not in the population. Hence, Setting
${}_0^{ABC}D_t^\sigma S(t) = 0, {}_0^{ABC}D_t^\sigma A(t) = 0, {}_0^{ABC}D_t^\sigma I(t) = 0, {}_0^{ABC}D_t^\sigma Q(t) = 0, {}_0^{ABC}D_t^\sigma R(t) = 0, {}_0^{ABC}D_t^\sigma B(t) = 0, A = 0, I = 0, Q = 0, B = 0$
in the cholera model (2), then computed cholera-free equilibrium is given by

$$\begin{cases} \Pi - \lambda_1\lambda_2 S - \mu S + \alpha R = 0, \\ (1-p)\lambda_1\lambda_2 S - (\varphi + \delta_1 + \mu + \xi)A = 0, \\ P\lambda_1\lambda_2 S - (\omega + \delta_2 + \mu + \xi)I = 0, \\ \varphi A + \omega I - (\theta + \delta_3 + \mu + \xi)Q = 0, \\ \theta Q - (\mu + \alpha)R = 0, \\ rB(1 - \frac{B}{K}) + \delta_1 A + \delta_2 I + \delta_3 Q - \mu_B B = 0. \end{cases} \tag{24}$$

Then the system of equations (22) is simplified, which gives
$\Pi - \lambda_1\lambda_2 S - \mu S + \alpha R = 0.$
By solving above equation we get,
$S_0 = \frac{\Pi}{\mu}$.
Therefore, our disease-free equilibrium point is $E_0 = (\frac{\Pi}{\mu}, 0, 0, 0, 0, 0)$.

4.2 Endemic Equilibrium

The endemic equilibrium point $E^* = (S^*, A^*, I^*, Q^*, R^*, B^*)$ of cholera model is the point where the infection persists in the Population or where rate of change of fractional derivatives vanish and it is obtained by solving the following equations:

$$\begin{cases} {}_0^{ABC}D_t^\sigma S(t) = 0, \\ {}_0^{ABC}D_t^\sigma A(t) = 0, \\ {}_0^{ABC}D_t^\sigma I(t) = 0, \\ {}_0^{ABC}D_t^\sigma Q(t) = 0, \\ {}_0^{ABC}D_t^\sigma R(t) = 0, \\ {}_0^{C}D_t^\sigma B(t) = 0. \end{cases} \tag{25}$$

$$\begin{cases} \Pi - \lambda_1\lambda_2 S - \mu S + \alpha R = 0, \\ (1-p)\lambda_1\lambda_2 S - (\varphi + \delta_1 + \mu + \xi)A = 0, \\ P\lambda_1\lambda_2 S - (\omega + \delta_2 + \mu + \xi)I = 0, \\ \varphi A + \omega I - (\theta + \delta_3 + \mu + \xi)Q = 0, \\ \theta Q - (\mu + \alpha)R = 0, \\ rB(1 - \frac{B}{K}) + \delta_1 A + \delta_2 I + \delta_3 Q - \mu_B B = 0. \end{cases} \tag{26}$$

Hence, the solution of preceding equation is given by

$$E^* = (S^*, A^*, I^*, Q^*, R^*, B^*), \tag{27}$$

where

$$\begin{cases} Q^* = (\mu + \alpha)R^*, \\ I^* = \frac{p\lambda_1\lambda_2 S^*}{\theta\delta_3 + \mu + \xi}, \\ B^* = K\frac{(r - r_B + \sqrt{(r-\mu_B)^2 + 4\frac{r}{K})(\delta_1 A^* + \delta_2 I^* \delta_3 Q^*))}}{2r}, \\ S^* = \frac{\alpha R^* + \Pi}{\lambda_1\lambda_2 + \mu}, \\ R^* = \frac{Q^*}{\mu + \alpha}, \\ A^* = \frac{(\theta + \delta_3 + \mu + \xi)Q^* - \omega I^*}{\omega}. \end{cases} \tag{28}$$

4.3 Basic Reproduction Number

Here, the threshold Parameter that governs the Spread of disease known as the basic reproduction number is obtained. It is nothing but the Spectral radius of the next-generation matrix. For the purpose, the System of model (3) is rearranged Starting with those representing newly infective classes:

$$\begin{cases} {}^{ABC}_{0}D^{\sigma}_{t}A(t) = (1-p)\lambda_1\lambda_2 S - (\varphi+\delta_1+\mu+\xi)A, \\ {}^{ABC}_{0}D^{\sigma}_{t}I(t) = P\lambda_1\lambda_2 S - (\omega+\delta_2+\mu+\xi)I, \\ {}^{ABC}_{0}D^{\sigma}_{t}Q(t) = \varphi A + \omega I - (\theta+\delta_3+\mu+\xi)Q, \\ {}^{C}_{0}D^{\sigma}_{t}B(t) = rB(1-\frac{B}{K}) + \delta_1 A + \delta_2 I + \delta_3 Q - \mu_B B. \end{cases} \tag{29}$$

Let $Z = [A, I, Q, B]^T$ denote a vector of infectious variables,then

$${}^{ABC}_{0}D^{\sigma}_{t}Z = F(Z) - V(Z) = \begin{bmatrix} (1-p)\lambda_1\lambda_2 S \\ p\lambda_1\lambda_2 S \\ \varphi A + \omega I \\ rB(1-\frac{B}{k}) + \delta_1 A + \delta_2 I + \delta_3 Q \end{bmatrix} - \begin{bmatrix} (\varphi+\delta_1+\mu+\xi)A \\ (\omega+\delta_2+\mu+\xi)I \\ (\theta+\delta_3+\mu+\xi)Q \\ \mu_B B \end{bmatrix},$$

with the next-generation matrices

$$F = \frac{\partial F(Z)}{\partial Z}|_{E_0} = \begin{bmatrix} \delta_1 & \delta_2 & \delta_3 & r \\ 0 & 0 & 0 & 0 \\ \varphi & \omega & 0 & 0 \\ 0 & 0 & 0 & 0 \end{bmatrix}, V^{-1} = \frac{\partial V(Z)}{\partial Z}|_{E_0} = \begin{bmatrix} \frac{1}{(\varphi+\delta_1+\mu+\xi)} & 0 & 0 & 0 \\ 0 & \frac{1}{(\omega+\delta_2+\mu+\xi)} & 0 & 0 \\ 0 & 0 & \frac{1}{(\theta+\delta_3+\mu+\xi)} & 0 \\ 0 & 0 & 0 & \frac{1}{(\mu_B)} \end{bmatrix},$$

which leads to

$$FV^{-1} = \begin{bmatrix} \frac{\delta_1}{(\varphi+\delta_1+\mu+\xi)} + \frac{\delta_2}{(\omega+\delta_2+\mu+\xi)} + \frac{\delta_3}{(\theta+\delta_3+\mu+\xi)} + \frac{r}{\mu_B} & 0 & 0 & 0 \\ 0 & 0 & 0 & 0 \\ 0 & 0 & 0 & 0 \\ 0 & 0 & 0 & 0 \end{bmatrix}, \quad \text{then,} \quad R_0$$

$$\begin{vmatrix} \frac{\delta_1}{(\varphi+\delta_1+\mu+\xi)} + \frac{\delta_2}{(\omega+\delta_2+\mu+\xi)} + \frac{\delta_3}{(\theta+\delta_3+\mu+\xi)} + \frac{r}{\mu_B} - \lambda & 0 & 0 & 0 \\ 0 & 0-\lambda & 0 & 0 \\ 0 & 0 & 0-\lambda & 0 \\ 0 & 0 & 0 & 0-\lambda \end{vmatrix} = 0,$$

Here, by the next generation matrix principle, the largest eigenvalue is the basic reproduction number.
Therefore, our basic reproduction number is

$$R_0 = \frac{\delta_1}{(\varphi+\delta_1+\mu+\xi)} + \frac{\delta_2}{(\omega+\delta_2+\mu+\xi)} + \frac{\delta_3}{(\theta+\delta_3+\mu+\xi)} + \frac{r}{\mu_B}. \tag{30}$$

4.4 Local Stability of Cholera Free Equilibrium

Theorem 5.*Cholera-free equilibrium E_0 of system of equations given in (1) is locally asymptotically stable if $R_0 < 1$ and unstable if $R_0 > 1$.*

*Proof.*To show that the CFE point of our model system 3 is locally asymptotically stable, we need to show that all the eigenvalues of Jacobian matrix J of system of Equation (3) evaluated at CFE point satisfies the condition $|arg(\lambda_i)| > \alpha\frac{\pi}{2}$. Let us find the Jacobian matrix J of model system of Equation (3) at CFE point. Jacobian matrix J of (3) evaluated at DFE point is given by

$$\begin{cases} {}^{ABC}_{0}D^{\sigma}_{t}S(t) = F_1(t,S) = g_1, \\ {}^{ABC}_{0}D^{\sigma}_{t}A(t) = F_2(t,A) = g_2, \\ {}^{ABC}_{0}D^{\sigma}_{t}I(t) = F_3(t,I) = g_3, \\ {}^{ABC}_{0}D^{\sigma}_{t}Q(t) = F_4(t,Q) = g_4, \\ {}^{ABC}_{0}D^{\sigma}_{t}R(t) = F_5(t,R) = g_5, \\ {}^{C}_{0}D^{\sigma}_{t}B(t) = F_6(t,B) = g_6. \end{cases} \tag{31}$$

Then the Jacobian matrix evaluated at E_0 becomes

$$J(E_0)=\begin{bmatrix} -\mu & 0 & 0 & 0 & \alpha & 0 \\ 0 & -(\varphi+\delta_1+\mu+\xi) & 0 & 0 & 0 & 0 \\ 0 & 0 & -(\omega+\delta_2+\mu+\xi) & 0 & 0 & 0 \\ 0 & \varphi & \omega & -(\theta+\delta_3+\mu+\xi) & 0 & 0 \\ 0 & 0 & \theta & 0 & -(\alpha+\mu) & 0 \\ 0 & \delta_1 & \delta_2 & \delta_3 & 0 & r(1-\frac{\Pi}{k})-\mu_B \end{bmatrix} \tag{32}$$

From equation(27) the eigenvalues are evaluated as follows:

$$J(E_0)=\begin{bmatrix} -\mu-\lambda & 0 & 0 & 0 & \alpha & 0 \\ 0 & -(m)-\lambda & 0 & 0 & 0 & 0 \\ 0 & 0 & -(n)-\lambda & 0 & 0 & 0 \\ 0 & \varphi & \omega & -(\theta+\delta_3+\mu+\xi)-\lambda & 0 & 0 \\ 0 & 0 & \theta & 0 & -(\alpha+\mu)-\lambda & 0 \\ 0 & \delta_1 & \delta_2 & \delta_3 & 0 & r(1-\frac{\Pi}{k})-\mu_B-\lambda \end{bmatrix} \tag{33}$$

where m=$\varphi+\delta_1+\mu+\xi$,n=$\omega+\delta_2+\mu+\xi$.
The characteristic polynomial of equation (28)becomes
$(-\mu-\lambda)(-(\varphi+\delta_1+\mu+\xi)-\lambda)(-(\omega+\delta_2+\mu+\xi)$
$-\lambda)(-(\theta+\delta_3+\mu+\xi)-\lambda)(-(\alpha+\mu)-\lambda)(r(1-\frac{\Pi}{k})-\mu_B-\lambda)=0.$
By factorizing the characteristic polynomial of equation,eigenvalues are as follows:
$\lambda_1=-\mu,\lambda_2=-(\varphi+\delta_1+\mu+\xi),\lambda_3=-(\omega+\delta_2+\mu+\xi),$
$\lambda_4=-(\theta+\delta_3+\mu+\xi),\lambda_5=-(\alpha+\mu,\lambda_6=-((r(1-\frac{\Pi}{k})-\mu_B)$
. Since
$\lambda_1<0,\lambda_2<0,\lambda_3<0,\lambda_4<0,\lambda_5<0,\lambda_6<0$ for r positive, know the sign of all eigenvalues are negative.
Therefore,our cholera-free equilibrium point is locally asymptotically stable if and only if $R_0<1$.

4.5 Global Stability of Cholera Free Equilibrium

Model(3) can be rewritten in the following form:

$$\begin{cases} \frac{dX}{dt}=H(X,Z), \\ \frac{dy}{dt}=G(X,Z), G(X,0)=0. \end{cases} \tag{34}$$

The cholera -free equilibrium E_0^1 of the preceding system is

$$E_0^1=(X^0,0),$$

where X^0 is the cholera-free equilibrium of the cholera-free system.
According to [19] ,to guarantee global asymptotic stability,we verify the following conditions H_1 and H_2 to be satisfied:

i.H_1: for $\frac{dX}{dt}=H(X,0)$,
X^0 is the globally asymptotically stable equilibrium.
ii.H_2: $G(X,Z)=PY-\hat{G}(X,Z),\hat{G}(X,Z)\geq 0$ for $(X,Z)\in\Omega$.

Here,$P=D_ZG(X,0)$ satisfy the condition of the Metzler matrix, and Ω is a region of feasible solutions.
Now,we state the following theorem.

Theorem 6.*The cholera-free equilibrium of the cholera dynamic model is globally asymptotically stable if $R_0<1$ if conditions H_1 and H_2 are satisfied and unstable whenever $R_0>1$.*

*Proof.*From model (3), we have

$$H(X,0) = \Pi - \mu S = H(S,0). \tag{35}$$

Solving $H(X,0) = 0$, we obtain $S = \frac{\Pi}{\mu}$.
Hence,$X^0 = (\frac{\Pi}{\mu}, 0)$.
Here, X^0 is the globally stable equilibrium of equation.

$$\frac{dX}{dt} = H(X,0). \tag{36}$$

From the infected compartments of model (3), we obtain

$$G(X,Z) = \begin{bmatrix} -(\varphi+\delta_1+\mu+\xi) & 0 & 0 & 0 \\ 0 & -(\omega+\delta_2+\mu+\xi) & 0 & 0 \\ \varphi & \omega & -(\theta+\delta_2+\mu+\xi) & 0 \\ \delta_1 & \delta_2 & \delta_3 & r-\mu_B \end{bmatrix} \begin{bmatrix} A \\ I \\ Q \\ B \end{bmatrix} - \begin{bmatrix} (1-P)\lambda_1\lambda_2 S \\ P\lambda_1\lambda_2 S \\ 0 \\ \frac{rB^2}{K} \end{bmatrix}$$

At the cholera -free equilibrium, the preceding equation reduces to the following form:

$$G(X,Z) = \begin{bmatrix} -(\varphi+\delta_1+\mu+\xi) & 0 & 0 & 0 \\ 0 & -(\omega+\delta_2+\mu+\xi) & 0 & 0 \\ \varphi & \omega & -(\theta+\delta_2+\mu+\xi) & 0 \\ \delta_1 & \delta_2 & \delta_3 & r-\mu_B \end{bmatrix} \begin{bmatrix} A \\ I \\ Q \\ B \end{bmatrix} - \begin{bmatrix} 0 \\ 0 \\ 0 \end{bmatrix}$$

$G(X,Z) = PY - \hat{G}(X,Z)$,
Where

$$P = \begin{bmatrix} -(\varphi+\delta_1+\mu+\xi) & 0 & 0 & 0 \\ 0 & -(\omega+\delta_2+\mu+\xi) & 0 & 0 \\ \varphi & \omega & -(\theta+\delta_2+\mu+\xi) & 0 \\ \delta_1 & \delta_2 & \delta_3 & r-\mu_B \end{bmatrix} \text{ and}$$

$$\hat{G}(X,Z) = \begin{bmatrix} 0 \\ 0 \\ 0 \end{bmatrix} \geq 0,$$

Now,it follows that the formulated model satisfied the hypothesis conditions required as
$G(X,Z) = PY - \hat{G}(X,Z)$,
where $\hat{G}(X,Z) \geq 0, \forall X,Z$.
Therefore, E_0 is globally asymptotically stable if $R_0 < 1$.

4.6 Global Stability of Endemic Equilibrium Point (EEP)

Theorem 7.*If $R_0 > 1$,then the endemic equilibrium point E^* of model (3) is globally asymptotically stable in the region Ω.*

*Proof.*Define a Lyapunov function candidate by
$F(S,A,I,Q,R) = \frac{1}{2}[(S-S^*)+(A-A^*)+(I-I^*)+(Q-Q^*)+(R-R^*)]^2$.
Then $F(S,A,I,Q,R) \geq 0$ and $F(S^*,A^*,I^*,Q^*,R^*) = 0$. Moreover,
$\frac{dF}{dt} = [(S+A+I+Q+R)-(S^*+A^*+I^*+Q^*+R^*)]\frac{dN}{dt}$.
Since
$S^*+A^*+I^*+Q^*+R^* = \frac{\Pi}{\mu}$
and
$\frac{dN}{dt} = \Pi - \mu N(t) - \delta_1 I - \xi A - \delta_2 I - \xi I, \delta_3 Q - \xi Q$,
we have
$\frac{dF}{dt} = (N - \frac{\Pi}{\mu})(\Pi - \mu N(t) - \delta_1 A - \xi A - \delta_2 I - \xi I) - \delta_3 Q - \xi Q)$
$= -\frac{1}{\mu}(\Pi - \mu N)^2 - (\Pi - \mu N)(\delta_1 A + \xi A + \delta_2 I + \xi I + \alpha_3 Q + \xi Q) \leq 0.$
Note that at the EEP we have $N \leq \frac{\Pi}{\mu}$.
Hence,it follows that $\frac{dF}{dt} \leq 0$ and $\frac{dF}{dt} = 0$ if and only if $S = S^*, A = A^*, I = I^*, Q = Q^*, R = R^*$.
Therefore the largest closed and bounded invariant set in

$$\{(S,A,I,Q,R,B) \in \Omega : \dot{F} = 0\}$$

is the set

$$\{E^* : E^* = (S^*, A^*, I^*, Q^*, R^*, B^*)\}.$$

By LaSalle's invariance principle the unique equilibrium point E^* is globally asymptotically stable when $R_0 > 0$ in the region Ω.

5 Numerical Results and Discussion

5.1 Numerical Results

In this Section, the principle Purpose is to Provide the Solution to the realistic version above, the use of the Adams-Moulton Numerical technique of the Atangana-Baleanu fractional integration, even as the values of this component are given withinside the paper [26].
The parameters presented in Table 1 are used in the simulation of solutions of SAIQR-B model and are either assumed or taken from the literature.

Table 1: Model Parameters Descriptions and Value

Symbols	parameters	Initial values	Reference
Π	recruitment rate	0.0002	Assumed
ξ	Cholera induced death rate	0.654	Assumed
δ	Rate of recovery using the available cholera treatment from $Q(t)$	0.437	Assumed
α_2	Rate of contribution from $Q(t)$ to $B(t)$	0.365	Assumed
β_1	Ingestion rate	0.235	Estimated
r	Intrinsic growth rate	0.0002	Estimated
θ	Rate of infected individuals join $Q(t)$ class	-0.125	Assumed
β_2	Transmission rate	-0.136	Assumed
α_1	Rate of contribution from $I(t)$ to $B(t)$	-0.459	Estimated
μ_B	Bacteria removal rate	-0.812	Estimated

$$\begin{cases} {}_0^{ABC}D_t^{\sigma} S = f_1(S(t_j), A(t_j), I(t_j), Q(t_j), R(t_j), B(t_j), t), \\ {}_0^{ABC}D_t^{\sigma} A = f_2(S(t_j), A(t_j), I(t_j), Q(t_j), R(t_j), B(t_j), t), \\ {}_0^{ABC}D_t^{\sigma} I = f_3(S(t_j), A(t_j), I(t_j), Q(t_j), R(t_j), B(t_j), t), \\ {}_0^{ABC}D_t^{\sigma} Q = f_4(S(t_j), A(t_j), I(t_j), Q(t_j), R(t_j), B(t_j), t), \\ {}_0^{ABC}D_t^{\sigma} R = f_5(S(t_j), A(t_j), I(t_j), Q(t_j), R(t_j), B(t_j), t), \\ {}_0^{ABC}D_t^{\sigma} B = f_6(S(t_j), A(t_j), I(t_j), Q(t_j), R(t_j), B(t_j), t), \end{cases} \tag{37}$$

where $0 < \sigma < 1$ and $t > 1$. Suppose one finds that the interval of the solution to the problem is [0,1]. The interval [0,1] is divided into N subintervals, each of which has length $h = \frac{n}{N}$. The nodes are $t_j = jh$ where $j = 0, 1, 2, ..., N$, and $t_{j+1} = t_j + h$. Thus, the generalized formula is

$$\begin{cases} S(t_{j+1}) = S(t_j) + \frac{1-\sigma}{G(\sigma)} f_1 + \frac{\sigma}{G(\sigma)} \sum_{N=0}^{\infty} (N+1)^{1-\sigma} - (N)^{1-\sigma} f_1, \\ A(t_{j+1}) = A(t_j) + \frac{1-\sigma}{G(\sigma)} f_2 + \frac{\sigma}{G(\sigma)} \sum_{N=0}^{\infty} (N+1)^{1-\sigma} - (N)^{1-\sigma} f_2, \\ I(t_{j+1}) = I(t_j) + \frac{1-\sigma}{G(\sigma)} f_3 + \frac{\sigma}{G(\sigma)} \sum_{N=0}^{\infty} (N+1)^{1-\sigma} - (N)^{1-\sigma} f_3, \\ Q(t_{j+1}) = Q(t_j) + \frac{1-\sigma}{G(\sigma)} f_4 + \frac{\sigma}{G(\sigma)} \sum_{N=0}^{\infty} (N+1)^{1-\sigma} - (N)^{1-\sigma} f_4, \\ R(t_{j+1}) = R(t_j) + \frac{1-\sigma}{G(\sigma)} f_5 + \frac{\sigma}{G(\sigma)} \sum_{N=0}^{\infty} (N+1)^{1-\sigma} - (N)^{1-\sigma} f_5, \\ B(t_{j+1}) = B(t_j) + \frac{1-\sigma}{G(\sigma)} f_6 + \frac{\sigma}{G(\sigma)} \sum_{N=0}^{\infty} (N+1)^{1-\sigma} - (N)^{1-\sigma} f_6, \end{cases} \tag{38}$$

where $f_i = (S(t_j), A(t_j), I(t_j), Q(t_j), R(t_j), B(t_j),)$,i=1,2,...,6.
Figure 2, based on the parameters in Table 1, visually demonstrates the local asymptotic stability of the disease-free equilibrium. The figure clearly shows the compartments S, A, I, Q, R, and B from top to bottom at t=50days, with the population labels indicating the corresponding numbers of individuals and bacteria.

In Figure 3, the effect of memory is illustrated by examining its impact on the growth of Vibrio cholerae in the environment. The stronger the memory effect, the greater the inhibition of bacterial growth. Higher Values of the fractional derivative show a more pronounced impact on the suppression of V. cholerae.

Figure 4 highlights the influence of the fractional derivative order on cholera recovery. The stronger the memory effect, the greater the number of individuals who recover from cholera with immunity. Additionally, as the fractional derivative order increases, the number of cholera-infected individuals decreases. The memory effect thus plays a crucial role in reducing the number of individuals who become infected with cholera.

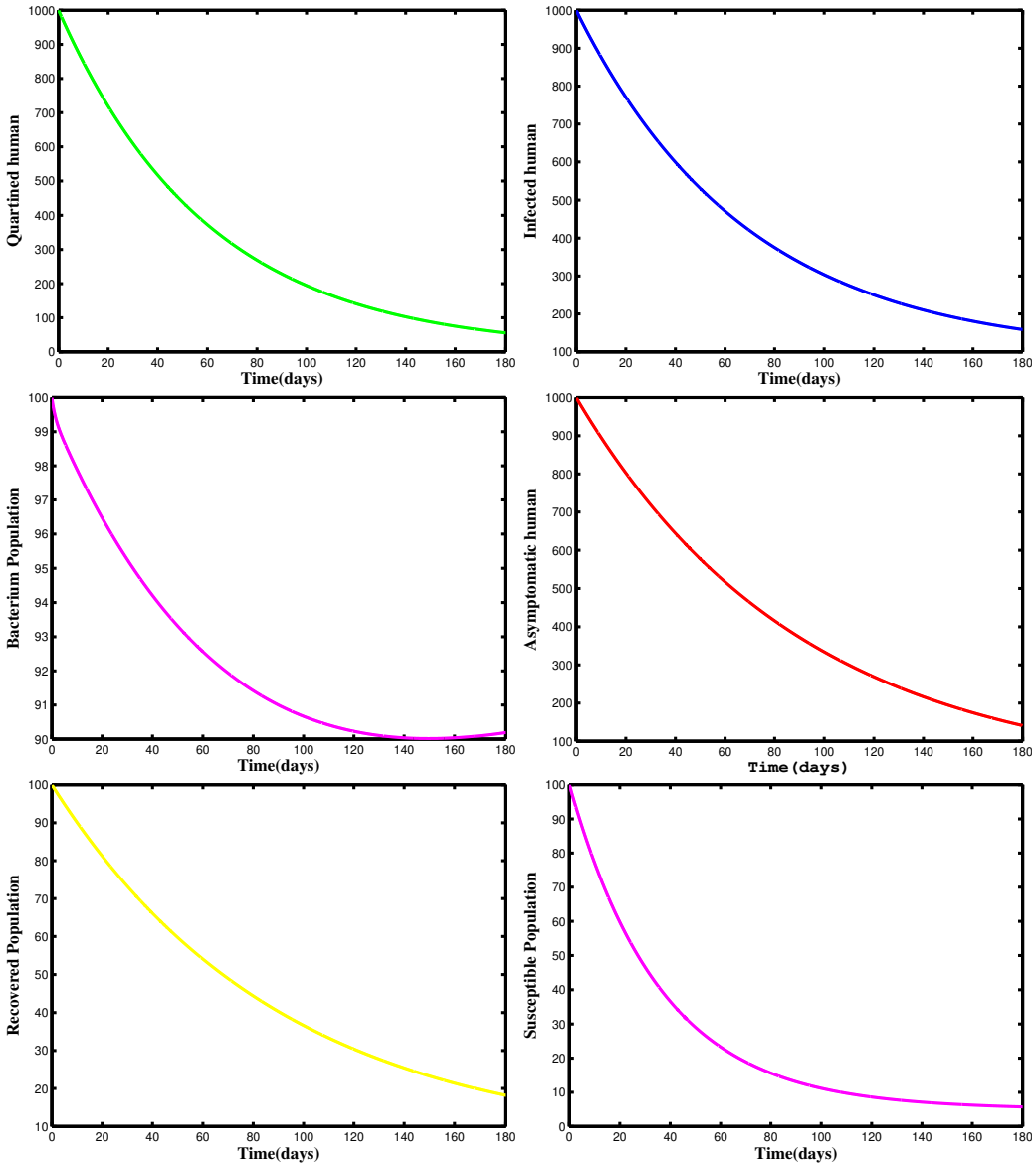

Fig. 2: Classical dynamical behavior of each state variable

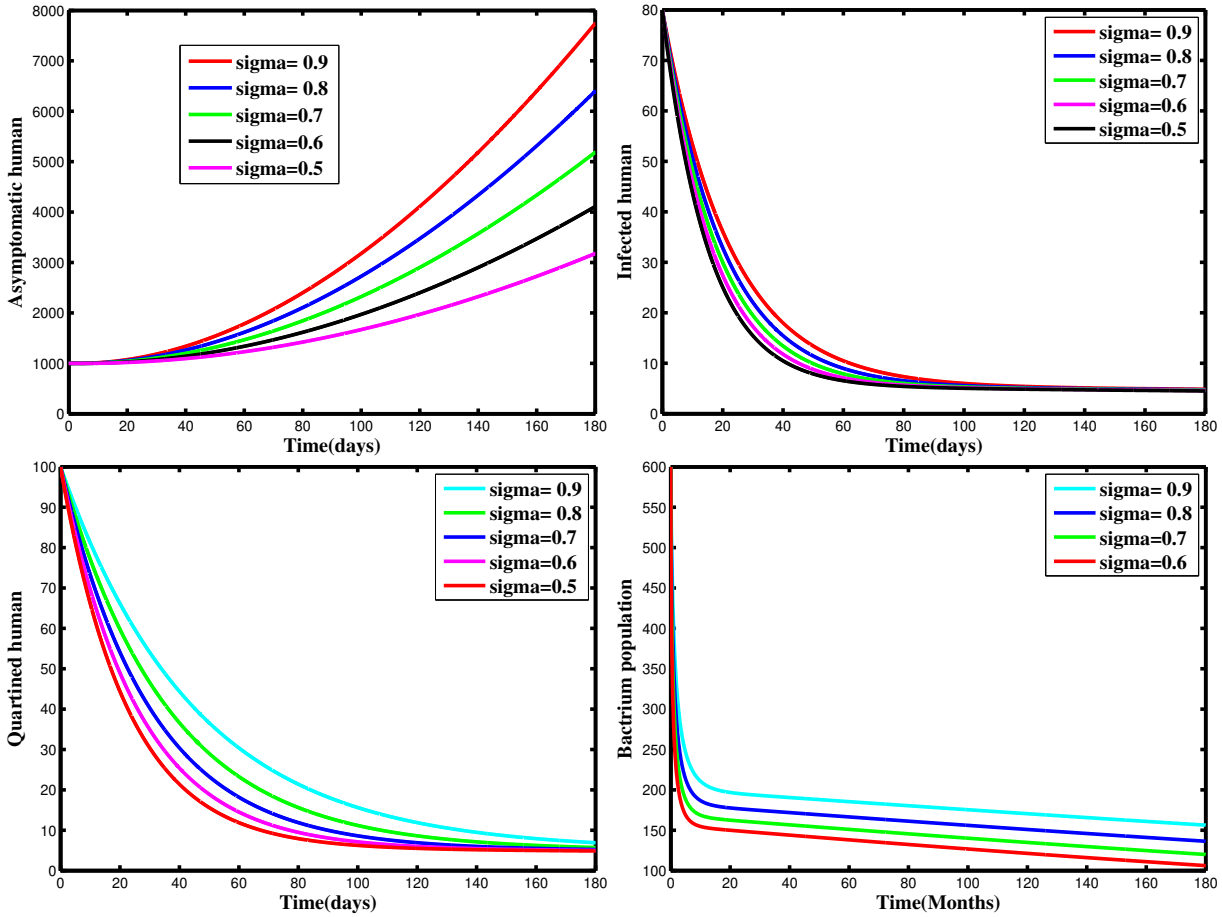

Fig. 3: ABC fractional-order dynamical behavior of disease control

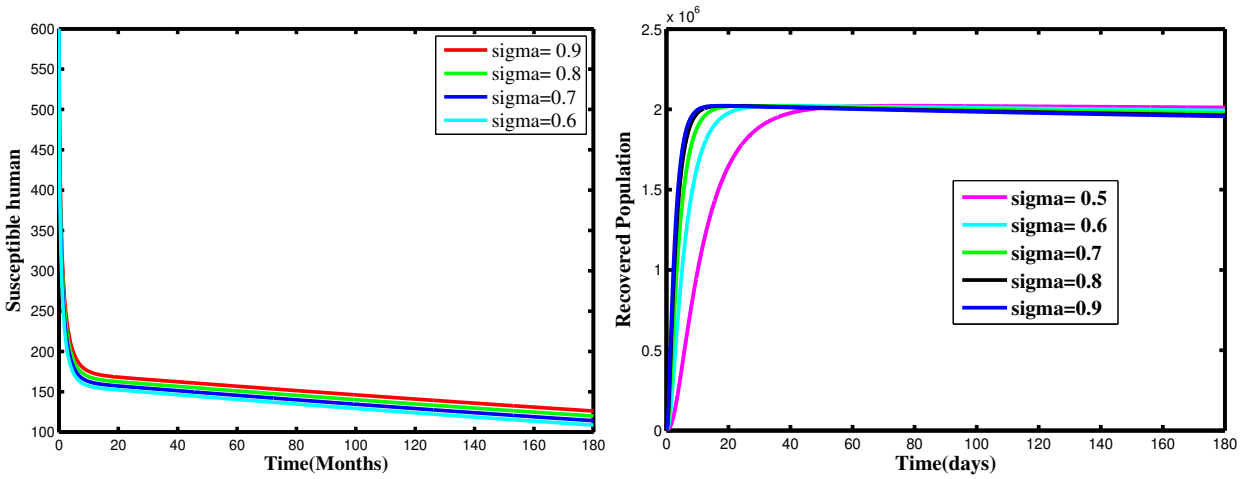

Fig. 4: Size of the susceptible and Recovered class over time for the system with different values of sigma at the disease free state where $R_0 < 1$

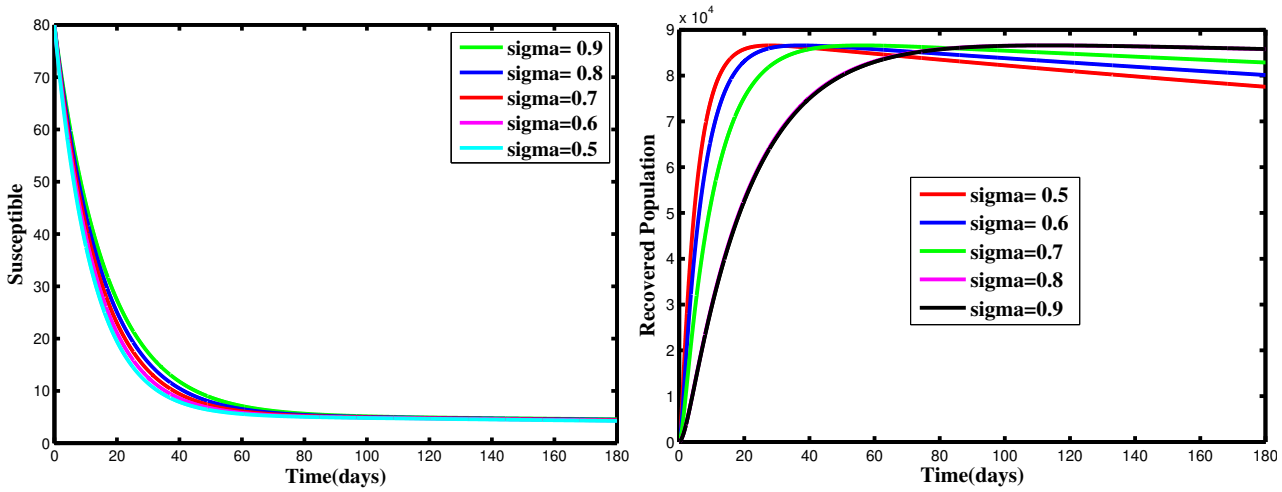

Fig. 5: Size of the susceptible and Recovered class over time for the system with different values of sigma at the disease free state where $R_0 > 1$

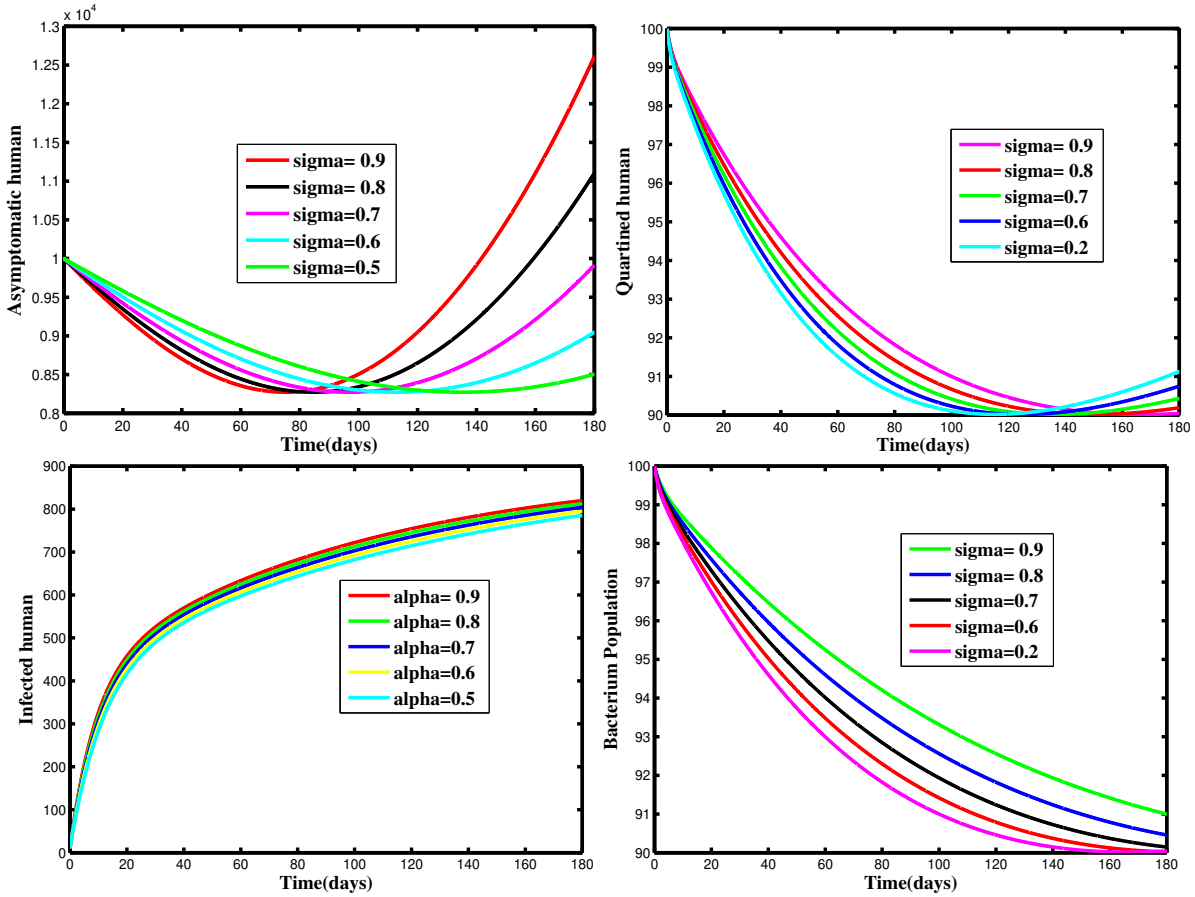

Fig. 6: Size of the Asymptomatic , Infected,Quarantined and Bacteria class over time for the system with different values of sigma at the disease free state where $R_0 < 1$

6 Conclusions

In this study, we developed and analyzed a SAIQR-B epidemic model incorporating the Atangana-Baleanu fractional derivative to explore the dynamics of cholera transmission. We carefully articulated the model assumptions and formulated a deterministic framework using systems of fractional-order differential equations. The model was analytically examined, and our analysis demonstrated that the solution to the fractional-order model remains bounded and non-negative within a positively invariant region. We also identified equilibrium points and calculated the basic reproduction number. Stability analyses of both the disease-free and endemic equilibrium points provided valuable insights into the local and global behavior of the system.

Using MATLAB simulations, we investigated the impact of memory effects on the cholera epidemic, particularly focusing on asymptomatic, infected, quarantined individuals, and the bacterium population under different fractional derivative orders. The findings from the simulations indicate that reducing the fractional derivative order from 1 results in a decline in the trajectory curves, leading to a slower reduction in the number of asymptomatic, infected, quarantined, and bacterium cases. As the fractional order decreases, the spread of the epidemic slows, and the peak number of cases in the susceptible and recovered compartments is reduced. Moreover, the results highlight the significant influence of memory on disease dynamics. Our comparison across various compartments suggests that decreasing the fractional derivative order could be an effective strategy for mitigating cholera outbreaks within communities.

The complex nature of cholera dynamics calls for further research, both biologically and mathematically. While modern fractional-order models, such as the one presented in this study, offer enhanced predictive capabilities over classical models, there remains substantial potential for further refinement. Despite those advancements, our findings strongly suggest that models incorporating fractional derivatives provide a more robust framework for understanding and controlling cholera transmission compared to those using ordinary derivatives.

Acknowledgment(s)

The authors would like to express their gratitude to the anonymous referees for their helpful recommendations that helped to enhance the nice of this paper.

Declarations

The authors declare that there is no conflict of interest with respect to the publication of this work.

Funding

This research received no specific funding from public, private, or non-profit funding agencies.

Data availability

The data we used for this study are from respective published and cited articles.

References

[1] Ganesan, D.; Gupta, S.S.; Legros, D. Cholera surveillance and estimation of burden of cholera. Vaccine 2020, 38, A13-A17. [CrossRef] [PubMed]
[2] Idoga, P.E.; Toycan, M.; Zayyad, M.A. Analysis of factors contributing to the spread of cholera in developing countries. Eurasian J. Med. 2019, 51, 121-127. [CrossRef] [PubMed]
[3] Atangana,A.,Baleanu, D,:New fractional derivatives with non local and non-singular kerner:theory and application to heat transfer model,Thermal Sci.20(2),763-769(2016).
[4] Llanes, R.; Somarriba, L.; Hern'andez, G.; Bardaj, Y.; Aguila, A.; Mazumder, R.N. Low detection of vibrio cholera carriage in healthcare workers returning to 12 Latin American countries from Haiti. Epidemiol. Infect. 2015, 143, 1016-1019. [CrossRef] [PubMed]
[5] Momba, M.; El-Liethy, M.A. Vibrio Cholerae and Cholera Biotypes; Global Water Pathogen Project: Pretoria, South Africa, 2018.

[6] Al-Refai and D. Baleanu,ON AN EXTENSION OF THE OPERATOR WITH MITTAG-LEFFLER KERNEL, Fractals, 30(51), 2022, Article number 2240129
[7] Javidi, M.; Ahmad, B. A study of a fractional-order cholera model. Appl. Math. Inf. Sci. 2014, 8, 2195-2206. [CrossRef]
[8] Lamond, E.; Kinyanjui, J. Cholera Outbreak Guidelines: Preparedness, Prevention and Control; Oxfam GB: Oxford, UK, 2012.
[9] Codeco, C. Endemic and epidemic dynamics of cholera: The role of the aquatic reservoir. BMC Infect. Dis. 2001, 1, 1-14. [CrossRef]
[10] MODIFIED ATANGANA-BALEANU FRACTIONAL DIFFERENTIAL OPERATORS, Ibrahim, R.W., Baleanu, D., Proceedings of the Institute of Mathematics and Mechanics, 48(Special Issue), 56-67 , 2022
[11] Hartley, D.M., Jr.; Morris, J.; Smith, D. Hyperinfectivity: A critical element in the ability of V. cholerae to cause epidemics? PLoS Med. 2006, 3, 63-69. [CrossRef] [PubMed]
[12] Mukandavire, Z.; Liao, S.; Wang, J.; Gaff, H.; Smith, D.; Morris, J. Estimating the reproductive numbers for the 2008-2009 cholera outbreaks in Zimbabwe. Proc. Natl. Acad. Sci. USA 2011, 108, 8767-8772. [CrossRef] [PubMed]
[13] Nelson, E.; Harris, J.; Morris, J.; Calderwood, S.; Camilli, A. Cholera transmission: The host, pathogen and bacteriophage dynamics. Nat. Rev. Microbiol. 2009, 7, 693-702. [CrossRef] [PubMed]
[14] Shuai, Z.; Tien, J.H.; Van den Driessche, P. Cholera models with hyper infectivity and temporary immunity. Bull. Math. Biol. 2012, 74, 2423-2445. [CrossRef]
[15] Shuai, Z.; van den Driessche, P. Modeling and control of cholera on networks with a common water source. J. Biol. Dyn. 2015, 9, 90-103. [CrossRef]
[16] Leo, J. Complexity of Epidemics Models: A Case-Study of Cholera in Tanzania. In Digital Transformation for Sustainability; Marx Gómez, J., Lorini, M.R., Eds.; Springer: Cham, Switzerland, 2022. [CrossRef]
[17] Lemos-Paião, A.; Silva, C.; Torres, D. A cholera mathematical model with vaccination and the biggest outbreak of world's history. AIMS Math. 2018, 3, 448-463. [CrossRef]
[18] Capasso, V.; Paveri-Fontana, S. A mathematical model for the 1973 cholera epidemic in the European Mediterranean region. Rev. D'epidémiologie Et De St. 1979, 27, 121-132.
[19] . Nishiura, H.; Tsuzuki, S.; Yuan, B.; Yamaguchi, T.; Asai, Y. Transmission dynamics of cholera in Yemen, 2017: A real time forecasting Theoret. Biol. Med. Model. 2017, 14, 14. [CrossRef]
[20] Neilan, R.; Schaefer, E.; Gaff, H.; Fister, K.; Lenhart, S. Modeling optimal intervention strategies for cholera. Bull. Math. Biol. 2010, 72, 2004-2018.
[21] Codeco CT. Endemic and epidemic dynamics of cholera: the role of the aquatic reservoir. BMC Infect Dis 2001;27:1-14.
[22] Yi W, Jinde C. Global dynamics of a network epidemic model for waterborne diseases spread. Appl Math Comput 2014;237:474-88.
[23] Yi W, Jinde C. Global stability of general cholera models with nonlinear incidence and removal rates. J Frankl Inst 2015;352:2464-85.
[24] Peter OJ, Ayoade AA, Abioye AI, Victor AA, Akpan CE. Sensitivity analysis of the parameters of a cholera model. J Appl Sci Environ Manag 2018;22:477-81.
[25] Mukandavire Z, Liao S, Wang J, Gaff H, Smith DL, Morris JG Jr. Estimating the reproductive numbers for the 2008-2009 cholera outbreaks in Zimbabwe. Proc Nat Acad Sci 2011;180:8767-72.
[26] Wang J, Modnak C. Modeling cholera dynamics with controls. Can Appl Math Quart 2011;19:255-73.
[27] Baleanu, D., Jajarmi, A., Mohammadi, H. and Rezapour, S. A new study on the mathematical modelling of human liver with Caputo-Fabrizio fractional derivative. Chaos, Solitons and Fractals, 134, 109705, (2020). [CrossRef]
[28] Losada, J. and Nieto, J.J. Properties of a new fractional derivative without singular kernel. Progress in Fractional Differentiation and Applications, 1(2), 87-92, (2015).
[29] Eustace, K.A., Osman, S. and Wainaina, M. Mathematical modelling and analysis of the dynamics of cholera. Global Journal of Pure and Applied Mathematics, 14(9), 1259-1275, (2018).
[30] Ferreira, C., Doursout, M.-F. J., & Balingit, J. S. (2023). Syphilis, cholera, and yellow fever. In 2000 years of pandemics: Past, present, and future (pp. 79-97). Springer.
[31] Avwerosuo, A. A., & Okedoye, A. M. (2023). Mathematical modelling of the dynamics and control of communicable diseases with emphasis on cholera epidemics. Asian Journal of Applied Science and Technology (AJAST), 7(4), 99-119.
[32] Baba, I. A., Humphries, U. W., & Rihan, F. A. (2023). A well-posed fractional order cholera model with saturated incidence rate. Entropy, 25(2), 360.
[33] Baleanu, D., Diethelm, K., Scalas, E., & Trujillo, J. J. (2012). Fractional calculus: models and numerical methods (Vol. 3). World Scientific.
[34] Bergounioux, M., & Bourdin, L. (2020). Pontryagin maximum principle for general caputo fractional optimal control problems with bolza cost and terminal constraints. ESAIM: Control, Optimisation and Calculus of Variations, 26, 35.
[35] Brumfield, K. D., Usmani, M., Chen, K. M., Gangwar, M., Jutla, A. S., Huq, A., & Colwell, R. R. (2021). Environmental parameters associated with incidence and transmission of pathogenic vibrio spp. Environmental microbiology, 23(12), 7314-7340.
[36] Cui, X., Xue, D., & Pan, F. (2022). A fractional svir-b epidemic model for cholera with imperfect vaccination and saturated treatment. The European Physical Journal Plus, 137(12), 1361.
[37] Duc, N. V., & Nguyen, T.-P. (2024). A regularization method for caputo fractional derivatives in the banach space l[0, t]. Numerical Algorithms, 95(2), 1033-1053.
[38] El Hayek, P., Boueri, M., Nasr, L., Aoun, C., Sayad, E., Jallad, K., et al. (2023). Cholera infection risks and cholera vaccine safety in pregnancy. Infectious Diseases in Obstetrics and Gynecology, 2023.

[39] Rautela, A., Bora, R. M., Dey, B. S., Paul, C. K., et al. (2023). Chemotherapy for cancer treatment: An l1 optimal control approach.
[40] Shackleton, D., Memon, F. A., Nichols, G., Phalkey, R., & Chen, A. S. (2023). Mechanisms of cholera transmission via environment in india and bangladesh: state of the science review. Reviews on Environmental Health(0).
[41] Wang, J. (2022). Mathematical models for cholera dynamicsa review. Microorganisms, 10(12), 2358.
[42] Yasmin, H., Aljahdaly, N. H., Saeed, A. M., & Shah, R. (2023). Investigating families of soliton solutions for the complex structured coupled fractional biswas-arshed model in birefringent fibers using a novel analytical technique. Fractal and Fractional, 7(7), 491.
[43] Christian Kuehn and Alexandra Neamt¸u. Center manifolds for rough partial differential equations. Electron. J. Probab., 28:Paper No. 48, 31, 2023.
[44] Mukandavire, Z., Garira, W. and Tchuenche, J.M. Modelling effects of public health educational campaigns on HIV/AIDS transmission dynamics. Applied Mathematical Modelling, 33(4), 2084-2095, (2009). [CrossRef]
[45] Layton, A.T. and Sadria, M. Understanding the dynamics of SARS-CoV-2 variants of concern in Ontario, Canada: a modeling study. Scientific Reports, 12, 2114, (2022). [CrossRef]
[46] Duran, S., Durur, H., Yavuz, M. and Yokus, A. Discussion of numerical and analytical techniques for the emerging fractional order murnaghan model in materials science. Optical and Quantum Electronics, 55, 571, (2023). [CrossRef]
[47] Sun, G.Q., Xie, J.H., Huang, S.H., Jin, Z., Li, M.T. and Liu, L. Transmission dynamics of cholera: mathematical modeling and control strategies. Communications in Nonlinear Scienceand Numerical Simulation, 45, 235-244, (2017). [CrossRef]
[48] Yokus, A., Durur, H., Kaya, D., Ahmad, H. and Nofal, T.A. Numerical comparison of Caputo and Conformable derivatives of time fractional Burgers-Fisher equation. Results in Physics, 25, 104247, (2021). [CrossRef]
[49] Ahmad, S., Dong, Q.I.U. and Rahman, M.U. Dynamics of a fractional-order COVID-19 model under the nonsingular kernel of Caputo-Fabrizio operator. Mathematical Modelling and Numerical Simulation with Applications, 2(4), 228-243, (2022). [CrossRef]
[50] Atede, A.O., Omame, A. and Inyama, S.C. A fractional order vaccination model for COVID-19 incorporating environmental transmission: a case study using Nigerian data. Bulletin of Biomathematics, 1(1), 78-110, (2023). [CrossRef]
[51] Ahmed, I., Yusuf, A., Sani, M.A., Jarad, F., Kumam, W. and Thounthong, P. Analysis of a Caputo HIV and malaria co-infection epidemic model. Thai Journal of Mathematics, 19(3), 897-912, (2021).
[52] Hanif, A., Butt, A.I.K., Ahmad, S., Din, R.U. and Inc, M. A new fuzzy fractional order model of transmission of Covid-19 with quarantine class. The European Physical Journal Plus, 136, 1179, (2021). [CrossRef]
[53] Joshi, H., Yavuz, M. and Stamova, I. Analysis of the disturbance effect in intracellular calcium dynamic on fibroblast cells with an exponential kernel law. Bulletin of Biomathematics, 1(1), 24-39, (2023). [CrossRef]
[54] T.L.Tirfe,L.L.Obsu and E.D.Gurmu,Mathematical modeling of cholera Dynamics and Analysis using Caputo fractional operator with optimal control,Progr.Fract.Differ.Appl.11,No.1,87-117(2025)
[55] A. Hanif, A. I. K. Butt, S. Ahmad,R. U. Din and M. Inc, A new fuzzy fractional order model of transmission of Covid-19 with quarantine class, Eur. Phys. J. Plus 136, 1179 (2021).
[56] A. O. Atede, A. Omame and S. C. A. Inyama, A fractional order vaccination model for COVID-19 incorporating environmental transmission: a case study using Nigerian data, Bull. Biomath. 1(1), 78-110 (2023).